Hindawi
International Journal of Polymer Science
Volume 2024, Article ID 1234797, 12 pages
https://doi.org/10.1155/2024/1234797

*Research Article*

# Experimental Investigation on the 3D Printing of Nylon Reinforced by Carbon Fiber through Fused Filament Fabrication Process, Effects of Extruder Temperature, and Printing Speed

**Mahmoud Moradi**,[1] **Zeinab Malekshahi Beiranvand**,[2] **Nahid Salimi**,[1] **Saleh Meiabadi**,[3] **and Jonathan Lawrance**[4]

[1]*Faculty of Arts, Science and Technology, University of Northampton, Northampton NN1 5PH, UK*
[2]*Department of Materials, Faculty of Engineering, Tarbiat Modares University, Tehran, Iran*
[3]*Department of Mechanical Engineering, École de technologie supérieure, 1100 Notre-Dame West, Montreal, QC, Canada H3C 1K3*
[4]*School of Computing, Engineering & Physical Sciences, University of the West of Scotland (UWS), High Street, Paisley PA1 2BE, UK*

Correspondence should be addressed to Mahmoud Moradi; mahmoud.moradi@northampton.ac.uk
and Zeinab Malekshahi Beiranvand; z.malekshahi.beiranvand@gmail.com

Received 30 December 2023; Revised 6 March 2024; Accepted 18 March 2024; Published 10 May 2024

Academic Editor: Vito Speranza



This study investigated how the extruder temperature, printing speed, and specimen geometry interact during a tensile test of continuous carbon fiber-reinforced nylon matrix composites produced by the fused deposition modelling (FDM) process. The investigation utilized statistical techniques. For this purpose, tensile examinations were done on manufactured samples using a testing apparatus. The study's objective is to identify the most efficient specimen geometry for tensile testing result optimization and to maximize the 3D printing process's capability for producing complex, freeform patterns in these composites. In this study, the input parameters required for the response surface methodology (RSM) were varying extruder temperature (240-255°C) and printing speed (60-80 mm/s), and experimental responses included modulus, elongation at break, and weight. The findings of the regression analysis showed output responses are influenced by both input variables. The results showed that the strength of the samples was significantly influenced by the input parameters. To draw the surface and residual plots, the software of design expert software was used. The interaction between the two input variables suggests raising the extruder temperature and decreasing printing speed, which leads to printing heavier samples. Inversely, the diversity between the forecasted and real responses for the optimal specimens is less than 10% which is assumed to be acceptable for the design of experiments (DOE). The analysis took into account the lower and upper ranges of the input variable with the goal of enhancing both the most modulus and fracture elongation while simultaneously degrading the weight of the specimens. To achieve this objective, the extruder temperature and printing speed are between 240 and 250°C and 65 and 75 mm/s, respectively.

## 1. Introduction

Recently, manufacturing processes have been one of the most important challenges in the industry. Accordingly, rapid prototyping (RP) technologies have appeared. This technique speeds up the manufacturing process on various scales [1, 2]. In the AM method, various materials such as metals, polymers, and composites can be produced layer by layer with the help of computer design [3, 4]. Laminated object manufacturing (LOM) and stereolithography (SLA) were the two first RP processes commercially available [5]. In the LOM process, physical prototypes are built by sequentially laminating, bonding, and cutting two-dimensional (2D) cross-sections generated by a CAD model [5]. The filament material extrusion is an extrusion process that deposits thermoplastic filaments through a hot nozzle tip and fills them in line, or curved strand forms, following a technological machine program. Stratasys Inc. first invented

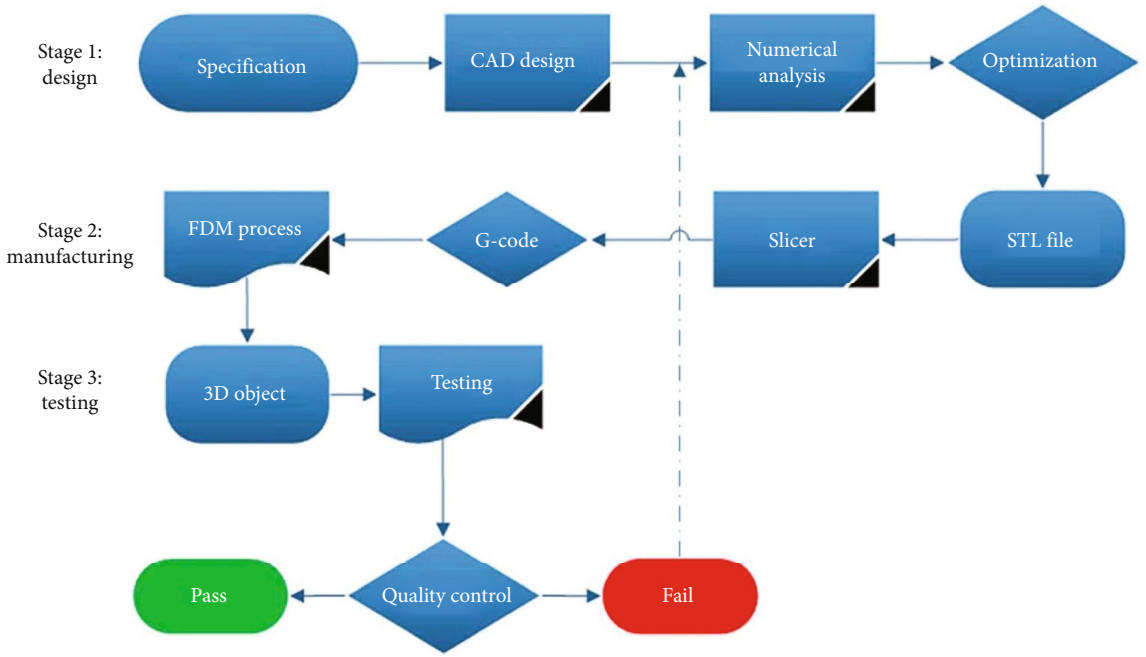


Figure 1: The methodology framework.

Table 1: Independent parameters accompanied by the levels of design.

| Independent parameter | Notation | Unit | -2 | -1 | 0 | 1 | 2 |
|---|---|---|---|---|---|---|---|
| Extruder temperature | ET | ˚C | 235 | 240 | 245 | 250 | 255 |
| Printing speed | BT | mm/s | 60 | 65 | 70 | 75 | 80 |

Table 2: Experimental layout and multiperformance results.

| Experiment no. | Input variables | | Output variables | | |
|---|---|---|---|---|---|
| | Extruder temperature (˚C) | Printing speed (mm/s) | Modulus (MPa) | Elongation (%) | Weight (g) |
| 1 | 245 | 80 | 17.68 | 7.79 | 10.28 |
| 2 | 250 | 65 | 23.08 | 4.46 | 10.17 |
| 3 | 245 | 60 | 24.30 | 3.77 | 10.14 |
| 4 | 245 | 70 | 26.37 | 4.72 | 10.18 |
| 5 | 245 | 70 | 24.76 | 7.87 | 9.96 |
| 6 | 235 | 70 | 26.53 | 2.71 | 10.21 |
| 7 | 255 | 70 | 25.22 | 2.92 | 9.27 |
| 8 | 240 | 65 | 23.15 | 3.33 | 9.18 |
| 9 | 240 | 75 | 26.36 | 2.86 | 9.29 |
| 10 | 245 | 70 | 24.14 | 2.58 | 9.2 |
| 11 | 250 | 75 | 26.08 | 4.53 | 10.83 |

the filament material extrusion process with the trade name fused deposition modelling (FDM), and later, this technology became popular for its open 3D printing systems as fused filament fabrication (FFF) technology [6]. Nowadays, the material extrusion process has become a trendy technology and is applied in various applications, including manufacturing complex, lightweight, and functional parts. The FFF process, in addition to its advantages, has some disadvantages, such as the surface quality, shape accuracy, and welding quality in

Table 3: CarbonX filament properties [33].

| Mechanical properties | FDM CarbonX |
|---|---|
| Elongation at break (ISO 527) | 3% |
| Tensile strength | 63 Mpa |
| Tensile modulus (ISO 527) | 3800 Mpa |
| Flexural strength (ISO 178) | 84 Mpa |
| Flexural modulus (ISO 178) | 3750 Mpa |

Table 4: Manufacturing parameters of FDM and their intended values.

| No. | Build parameters | Unit | Value | Definitions |
|---|---|---|---|---|
| 1 | Nozzle diameter | mm | 0.4 | It is the diameter of the extruder nozzle |
| 2 | Extrusion width | mm | 0.4 | Single outline width of the plastic extrusion |
| 3 | Build orientation | ° | 45 | The angle between the central axis and the horizontal direction |
| 4 | Build pattern | — | Triangular | It is the build pattern of the specimen |
| 5 | Infill density | % | 20 | It is the amount of material content |

brief [6]. Quality metrics of the FFF 3D printed parts as time, quality, and flexibility are also crucial for the well-being of the production of the elements [7]. It is essential to choose the correct parameters to prepare the models that will print. Careful choices must be made during this preproduction phase because it determines how right and sustainable the final product will be [7].

So far, various types of additive manufacturing methods have been developed, such as selective laser sintering (SLS) [8], selective laser melting (SLM) [9–11], and FDM [12]. Compared to other AM methods, the FDM technique is widely used due to its excellent characteristics such as low cost, easy operation, high accuracy and repeatability, and dimensional stability. Currently, this technique is introduced as an attractive subject in researches, highlighting the FDM methods' characteristics analytically and experimentally. Considering the literature [13], the significant topic in the field of FDM is examining manufacturing parameters' impact on mechanical characteristics and optimization techniques to obtain the best properties. Appropriate researches have been performed in other fields like numerical analysis [14, 15]. The significant effect of printing parameters on the properties of the final manufactured component and the use of novel geometric parameters. A key challenge in manufacturing composite components via this method is to find the relationship between the mechanical characteristics of the parts and the process parameters [16].

Continuous carbon fiber-reinforced nylon matrix composites have been widely used in various applications due to their high strength-to-weight ratio and excellent durability. In the past, the production of these specimens has been limited by the use of traditional manufacturing methods, which are not capable of producing complex shapes. The advent of 3D printing technology has opened up new possibilities in the production of these specimens, enabling the creation of optimal mechanical characteristics [17]. Many studies on the development of new composite materials using natural fiber as a feedstock filament for FDM have recently been published [18]. The mechanical behavior of FDM 3D-printed carbon fiber-strengthened composites was examined to give a premise for their plan and application in different areas [19]. The effect of the process parameters on the mechanical execution of the 3D printed ceaseless carbon fiber-strengthened thermoplastic composite sandwich structure and its potential for different applications requiring tall firmness and load-bearing capability were examined experimentally and computationally to improve the progression of modern, high-performance composite structures [20]. In a study, the effect of 3D printing

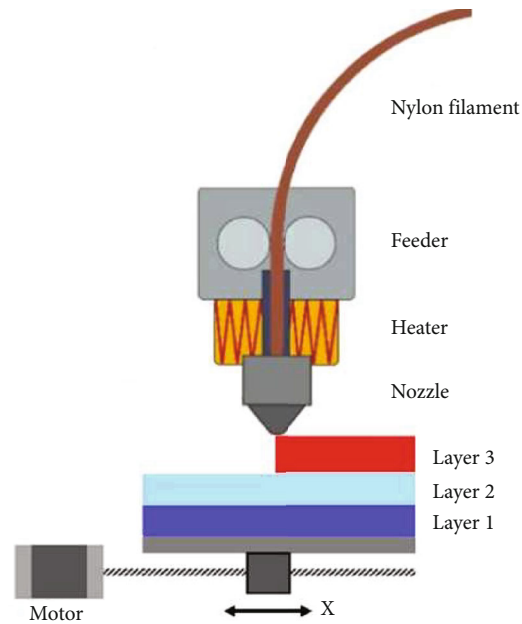


Figure 2: Principle of FDM process and output layers [22].

technology on the mechanical characteristics, tensile strength, and failure processes of 3D printed continuous carbon fiber-reinforced composites using various tab patterns was assessed to provide optimizing design and processing for diverse applications [21, 22]. The findings of a research study improved the performance of composites by optimizing the surface and understanding the underlying process [23]. The numerous operational variables that impact the mechanical behavior of composites, such as fiber type, fiber orientation, fiber volume fraction, printing settings, and postprocessing processes, were considered in a study to comprehend the constraints and opportunities of 3D printing technology in the production of fiber-reinforced polymer nanocomposites [24, 25]. In another research study, it was examined several types of infill-patterns (IPs) to manufacture fused deposition modelling (FDM) components considering improving mechanical properties such as tensile strength, elongation, and Young's modulus and the impact of IPs on them. An experimental setup was done, and tensile tests were performed to calculate mechanical responses [26]. The part produced by 3D printing has its accuracy varies with the changes in the process parameters of the machine such as quality, temperature, and speed. Taguchi method was applied in order to achieve the optimum accuracy of the printed part [27].

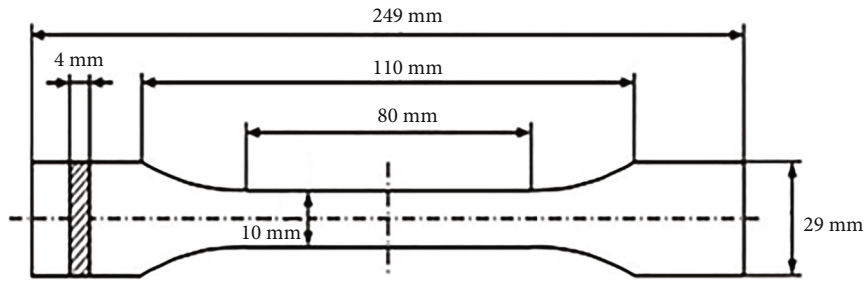


(a)

(b)

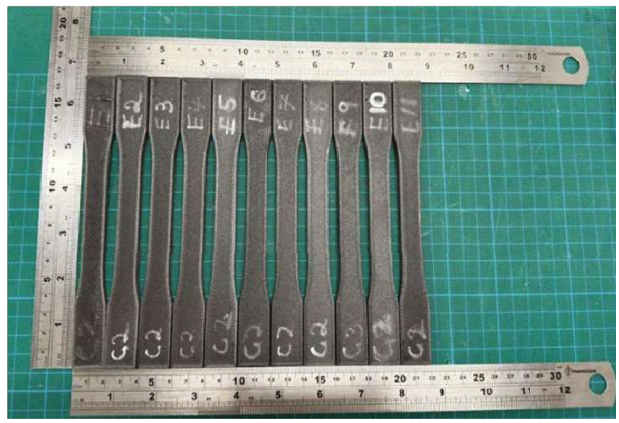

(c)

Figure 3: (a) 2D specimen with dimension. (b) Weighing of specimen. (c) Printed parts.

In the present study, a systematic experimental analysis is designed and manufactured for FDM parts to examine the impact of printing setting including extruder temperature and printing speed on the mechanical characteristics of continuous carbon fiber-reinforced nylon matrix composites. One of the most critical parameters affecting the mechanical properties of printed parts is the printing setting parameters. Therefore, the focus is placed on comparing the mechanical properties of printed samples based on various process parameters. The findings of this study will contribute to the development of the composite material industry by informing the design and manufacture of these composites for a variety of applications. In addition, they will be helpful in understanding the link between the mechanical characteristics of continuous carbon fiber-reinforced nylon matrix composites and process parameters. The project is crucial because it aims to make use of 3D printing's potential for producing these composites in freeform designs. The specimens will go through tensile testing to establish their mechanical characteristics, including their tensile strength, elastic modulus, and elongation at break. Then, data from the tensile testing will be statistically examined. In this study, a comprehensive experimental and analytical examination of process parameters on specific mechanical responses of FDM parts is done. Also, the response surface method was conducted to optimize the weight, maximum modulus, and elongation of the manufactured specimens. The aim of the study is to improve the weight efficiency and mechanical properties of specimens produced by 3D printing.

## 2. Methodological Framework and Experiments

*2.1. Methodological Framework.* Statistical modelling is employed to determine the correlation between the parameters of the process, material characteristics, and the quality of the manufactured samples. It leads to optimizing the process parameter settings to obtain desired outcomes. In addition, mathematical optimization is utilized to find the main feasible solution within a complex of limitations. In 3D printing, this technique uses formulizing an objective function to determine the best optimal amounts of the parameters and the combination of process parameters that maximize or minimize the objective function. Responses were modelled and analysed by means of the statistical technique called RSM [28, 29]. The aim of RSM is to get the desired collection of variables that presents the most (or less) response [30, 31]. RSM has a broad span of usages, including control, and the optimization of the process [32]. Figure 1 shows the methodology flowchart including design, manufacturing, and testing.

The independent parameters with design levels are given in Table 1. Design levels are directed to the values allocated to a factor in an empirical scheme. This RSM scheme contains a centre spot (extruder temperature: 245°C; printing speed: 70 mm/s) which is iterated threefold to specify the inconsistency and prepare a prediction of the empirical error. Moreover, the design software gives a fractional factorial design to analyse the significant effects of the variables at yield levels suggesting 8 experimental tests. The number of

experiments with two variables and 5 levels is 11 (including 3 replications at the centre point and 8 factorial points). Table 2 provides the input parameters, responses, and the relative error of model predictions.

*2.2. Experimental Work.* The parameters of the CarbonX (Gen3) PA6 carbon fiber-reinforced nylon filament that was utilized are shown in Table 3. As shown in Table 4, the parameters including nozzle diameter, extrusion width, build orientation, build pattern, and infill density are constant parameters as the preset printing settings. The value and explanation of these parameters are described in Table 4.

Eleven samples of tensile test were created and manufactured using 3D printing with a totally triangular fiber pattern in accordance with the DOE results (Table 2) and fixed printing settings (Table 3). Figure 2 depicts the fundamentals of the FDM procedure using CarbonX (Gen3) PA6 carbon fiber-reinforced nylon filament as well as descriptions of the printing settings. Designing samples and defining material attributes as construction factors required the use of the simplified 3D program. Printing of the uniaxial tensile test followed ASTM-D 638. Figure 3 depicts the dimensions of both 3D printed samples and tensile test samples made in accordance with ASTM-D638. The Instron tensile testing machine was utilized to perform tensile tests at a speed of 5 mm/min (Figure 4). The printed examples feature nondense cores with varying densities and 20%-density shells. The infill density is therefore equal to the core density, and the number of contours is equal to the number of dense shells.

Elongation during break (%), part weight (g), building time (ms), and maximum fracture load (N) were chosen as the output parameters. The process of measurement was regarded as a normal circumstance. To do this, a digital timer determined the construction time after printing each sample, and a precision weighing scale determined the weight of the part. Tensile test also captured technical analysis such as maximum fracture load and break elongation. It should be mentioned that the software decided the programmed weight after calculating the geometric parameters. After a destructive test over a universal testing device, the FDM-produced specimens are displayed in Figure 5. With the specimen being loaded, material fibers tend to shift their path towards the loading direction because the strength and adhesion between fibers are exceeded by the tensile strength of the material fibers. The more fibers are towards the tensile direction in the tensile direction, the greater the extension at fracture for the sample specimens.

Figure 4: Instron tensile testing machine.

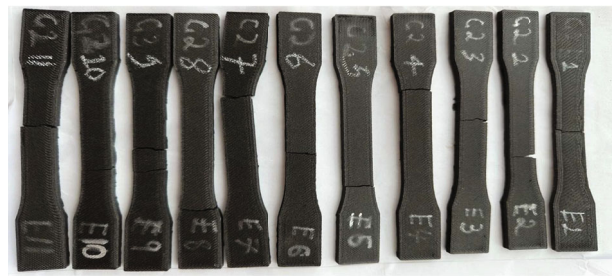

Figure 5: Specimens after tensile testing.

## 3. Result and Discussion

A statistical technique called analysis of variance (ANOVA) is used to compare differences between various groups. It determines if an average difference between two or more groups is meaningful or merely coincidental. The means of three or more independent groups are compared using an ANOVA to see if there is a statistically significant difference between them. Which groups are significantly different from one another and which groups are not can be determined using the outcomes of an ANOVA. The specimens were affixed to the tensile testing machine and subjected to elongation. The resulting output parameters, including Young's modulus, fracture elongation, and the weight, were obtained for the optimization The input and output parameters are shown in Table 2.

*3.1. Modulus of Elasticity (MPa).* The comparison of the effects of extruder temperature and printing speed on the modulus of elasticity in 3D printing may reveal that while neither factor is very important on its own, printing speed is more important than extruder temperature. The findings of an ANOVA can be used to draw this conclusion; they

Table 5: Analysis of variance table of modulus.

| Source | Sum of squares | Df | Mean square | $F$ value | $p$ value prob > $F$ |
|---|---|---|---|---|---|
| Model | $1.438 \times 10^8$ | 6 | $2.397 \times 10^7$ | 8.69 | 0.0094 |
| A-ET | $2.955 \times 10^6$ | 1 | $2.955 \times 10^6$ | 1.07 | 0.3405 |
| B-PS | $3.892 \times 10^7$ | 1 | $3.892 \times 10^7$ | 14.11 | 0.0094 |
| AB | 49562.04 | 1 | 49562.04 | 0.018 | 0.8977 |
| $A^2$ | $1.930 \times 10^6$ | 1 | $1.930 \times 10^6$ | 0.7 | 0.4349 |
| $B^2$ | $5.619 \times 10^7$ | 1 | $5.619 \times 10^7$ | 20.37 | 0.0040 |
| $A^2B$ | $6.78 \times 10^7$ | 1 | $6.78 \times 10^7$ | 24.61 | 0.0026 |
| Residual | $1.655 \times 10^7$ | 6 | $2.758 \times 10^6$ | | |
| Lack of fit | $8.204 \times 10^5$ | 2 | $4.102 \times 10^5$ | 0.10 | 0.9033 |
| Pure error | $1.573 \times 10^7$ | 4 | | | |
| Cor total | $1.604 \times 10^8$ | 12 | $3.932 \times 10^6$ | | |
| $R$-squared | 0.8968 | | $R$-squared (adj) | 0.7936 | |

show that while there is no significant difference in the means of modulus based only on extruder temperature between groups, there is a significant difference in the means of modulus based on printing speed. This shows that printing speed, as opposed to extruder temperature, has a bigger effect on the modulus of 3D-printed components. The ANOVA (Table 5) prepares invaluable visions into the impressive variables in the additive manufacturing of CarbonX (Gen3) PA6 carbon fiber-reinforced nylon specimens and their relative impacts. This table highlights the primary parameters that mainly affect the results of the manufacturing. Equation (1) displays the regression model, incorporating coefficients of input variables in the manufacturing. Analyzing the magnitudes of coefficients (derived from Eq. (1)) allows for the identification of which input variables exert a substantial influence on the outcome parameters. A positive coefficient shows that an increase in the input variable leads to an increase in the response parameter, whereas a negative coefficient shows that an increase in the input variable results in a reduction in the response parameter.

$$\begin{aligned}(\text{Modulus})^3 = {} & (-1.69194E + 008) + ((1.37884E + 006) \times \text{ET}) \\ & + ((2.43198E + 006) \times \text{PS}) \\ & - (19780.47147 \times \text{ET} \times \text{PS}) \\ & - \left(2813.53560 \times \text{ET}^2\right) \\ & - \left(62.63737 \times \text{PS}^2\right) \\ & + \left(40.35922 \times \text{ET}^2 \times \text{PS}\right).\end{aligned} \tag{1}$$

Figure 6 illustrates the response surface plot of modulus output concerning printing speed and extruder temperature.

*3.2. Elongation (mm) at Fracture.* When extruder temperature and printing speed are compared for their effects on elongation (a measure of a material's capacity to stretch), it may be discovered that extruder temperature has a greater impact on elongation than printing speed. The results of

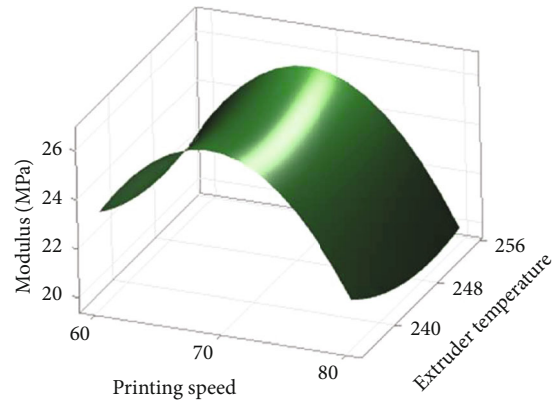


Figure 6: Response surface plot related to modulus output versus printing speed and extruded temperature.

an ANOVA (Table 6) can be used to draw this conclusion; they show that while the means of elongation based only on printing speed do not significantly differ across groups, the means based on extruder temperature do significantly differ. This shows that extruder temperature rather than printing speed has a stronger effect on the elongation of 3D-printed items. This shows no significant factor is affecting between printing speed and extruder temperature since the $p$ values are more than 0.05. But if we compare printing speed and extruder temperature among themselves, the extruder temperature has more significance than printing speed.

$$\begin{aligned}(\text{Fracture elongation})^{-0.76} = {} & +96.32072 - (0.77927 \times \text{ET}) \\ & + \left(1.58118E - 003 \times \text{ET}^2\right).\end{aligned} \tag{2}$$

When analyzing the manufactured specimens, evaluating the fracture elongation is critical as it enables the assessment of the specimens' ability to elongate before reaching the point of failure. In this study, the ANOVA identified

Table 6: Analysis of variance of elongation at fracture.

| Source | Sum of squares | Df | Mean square | $F$ value | $p$ value prob > $F$ |
|---|---|---|---|---|---|
| Model | 0.043 | 2 | 0.021 | 3.09 | 0.0904 |
| A-ET | $5.997 \times 10^{-3}$ | 1 | $5.997 \times 10^{-3}$ | 0.87 | 0.3742 |
| $A^2$ | 0.037 | 1 | 0.037 | 5.31 | 0.0440 |
| Residual | 0.069 | 10 | $6.93 \times 10^{-3}$ | | |
| Lack of fit | 0.020 | 6 | $3.411 \times 10^{-3}$ | 0.28 | 0.9198 |
| Pure error | 0.049 | 4 | 0.012 | | |
| Cor total | 0.11 | 12 | | | |
| $R$-squared | 0.3816 | | $R$-squared (adj) | 0.2580 | |

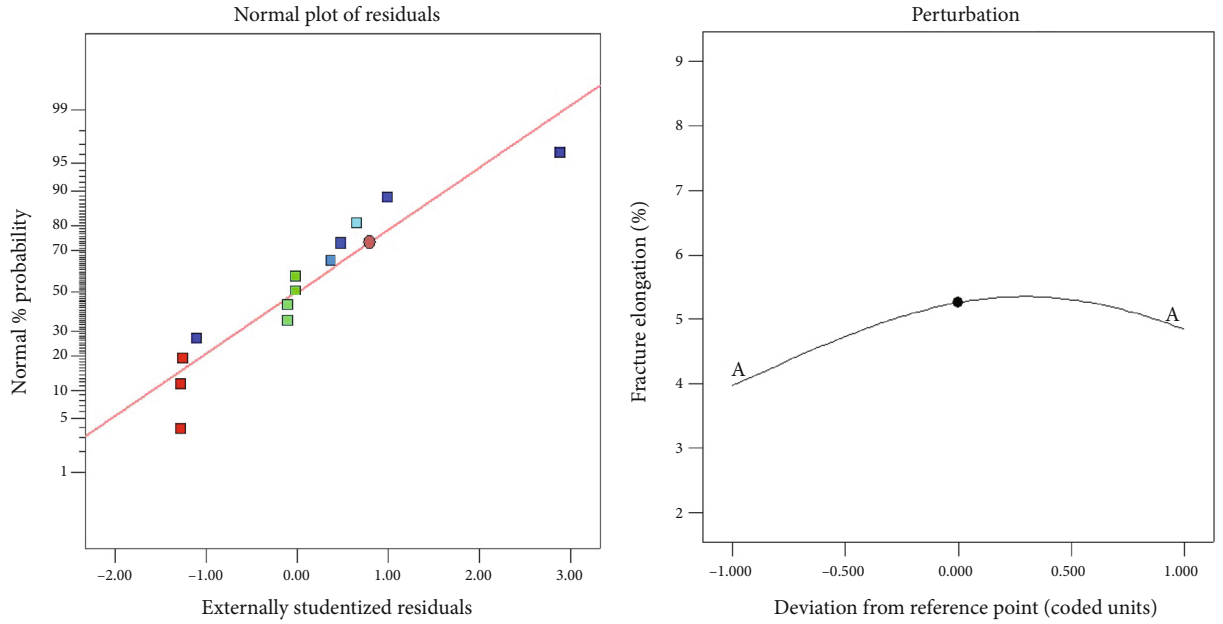


Figure 7: (a) Normal residual plot. (b) Perturbation plot.

the principal variables in the manufacturing process. Equation (2) generates coefficients of the input variable and the interaction coefficients which are critical in constructing the regression model providing the role of each input variable and their interactions on the fracture elongation. This permits an excellent comprehension of how different parameters impact the mechanical characteristics of the manufactured specimens. Furthermore, these coefficients can be employed to ascertain the best parameters of the input variables, leading to the maximum fracture elongation. Based on the analysis of the regression model, akin to the methods in the design experts V11 program, it is viable to identify the optimal magnitude. As shown in Eq. (2), the normal residuals plot (Figure 7(a)) and perturbation graphs (Figure 7(b)) were created to examine the sufficiency of the regression model and the precision of the predicted elongation values at break. The normal residuals plot prepares visions into the residual distribution and leads validation provided that the deviations from normality in the plot of the regression model assumptions show ability issues with the model's outcomes. The perturbation graphs in Figure 7(b) demonstrate the impact of the input variable on the fracture elongation. The graphs provide the reconnaissance of the significant parameters that mainly affect the response parameter. The value and direction of the perturbation show that the effect of the variable on the fracture elongation is able to be identified. Figures 8(a) and 8(b) show the effect of the IP on the fracture elongation. Increasing the IP causes more printing of PVA, leading to a higher elongation. This correlation is related to the raised length of the sample as more material is deposited. It gives adjusting input parameters, like printing speed, a main effect on the elongation characteristics of the manufactured specimens. With this understanding, researchers optimized the printing process by carefully adjusting the input variables to obtain the desired elongation levels preserving other quality properties.

*3.3. Weight.* The ANOVA (Table 7) for the part weight (g) versus printing speed and extruder temperature reveals that

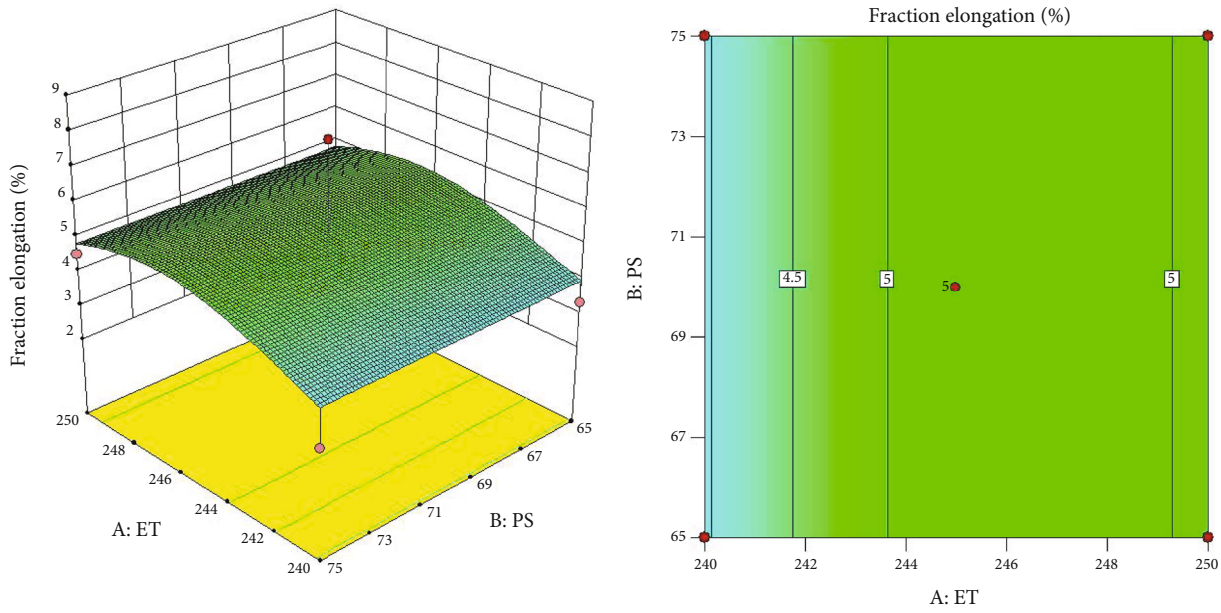


Figure 8: (a) The plot of response surface for fracture elongation output versus IP and pattern. (b) Contour illustrating the interaction between plot IP and pattern.

Table 7: Analysis of variance for part weight.

| Source | Sum of squares | Df | Mean square | $F$ value | $p$ value prob > $F$ |
|---|---|---|---|---|---|
| Model | $2.874 \times 10^5$ | 5 | 57485.53 | 6.80 | 0.0129 |
| A-ET | 35840.82 | 1 | 35840.82 | 4.24 | 0.0785 |
| B-PS | 1115.75 | 1 | 1115.75 | 0.13 | 0.7272 |
| AB | 198.03 | 1 | 198.03 | 0.023 | 0.8827 |
| $B^2$ | 17422.47 | 1 | 17422.47 | 2.06 | 0.1943 |
| $A^2B$ | $2.533 \times 10^5$ | 1 | $2.533 \times 10^5$ | 29.95 | 0.0009 |
| Residual | 59203.39 | 7 | 8457.63 | | |
| Lack of fit | 7552.64 | 3 | 2517.55 | 0.19 | 0.8948 |
| Pure error | 51650.75 | 4 | 12912.69 | | |
| Cor total | $3.466 \times 10^5$ | 12 | | | |
| $R$-squared | 0.8292 | | $R$-squared (adj) | 0.7072 | |

there is no significant factor, but among extruder temperature and printing speed, printing speed is more significant. This table gives us an idea of how the printing speed and extruder temperature play a role in affecting part weight. If a significant difference exists between the means of various combinations of printing speed and extrusion temperature on component weight, it can be determined using an ANOVA. A significant difference in the ANOVA findings indicates that there is no chance effect and that the effect of one or both of the parameters (printing speed and extrusion temperature) on component weight is real.

$$\begin{aligned}(\text{Weight})^3 = {} & (-2.95554E + 006) + (12088.01049 \times \text{ET}) \\ & + (84494.69355 \times \text{PS}) - (345.47276 \times \text{ET} \times \text{PS}) \\ & - \left(603.02722 \times \text{PS}^2\right) + \left(2.46565 \times \text{ET} \times \text{PS}^2\right).\end{aligned} \tag{3}$$

Figure 9(a) indicates the normal plot of residuals which are closely aligned with the red line showing that the residuals follow a normal distribution, confirming the assumptions of the regression analysis, adequately obtaining the inherent variability in the data, and providing well-founded estimates for the weight. The spike in Figure 9(a) that drifts notably from the style is an outlier suggesting that the anticipated model for weight is not robust enough to predict such extreme values. Figure 9(b) illustrates the perturbation graph of the process parameters on the weight of the parts. By investigating the value and direction of the perturbation lines, the effect of these variables on the weight can be assessed. The graph indicates that increasing the value of the input parameter reduces the weight of the sample. Determining the impact of variables on the weight of specimens is critical for obtaining desirable weight in manufactured parts. It is possible to qualify and adjust the weight of the manufactured specimens by carefully

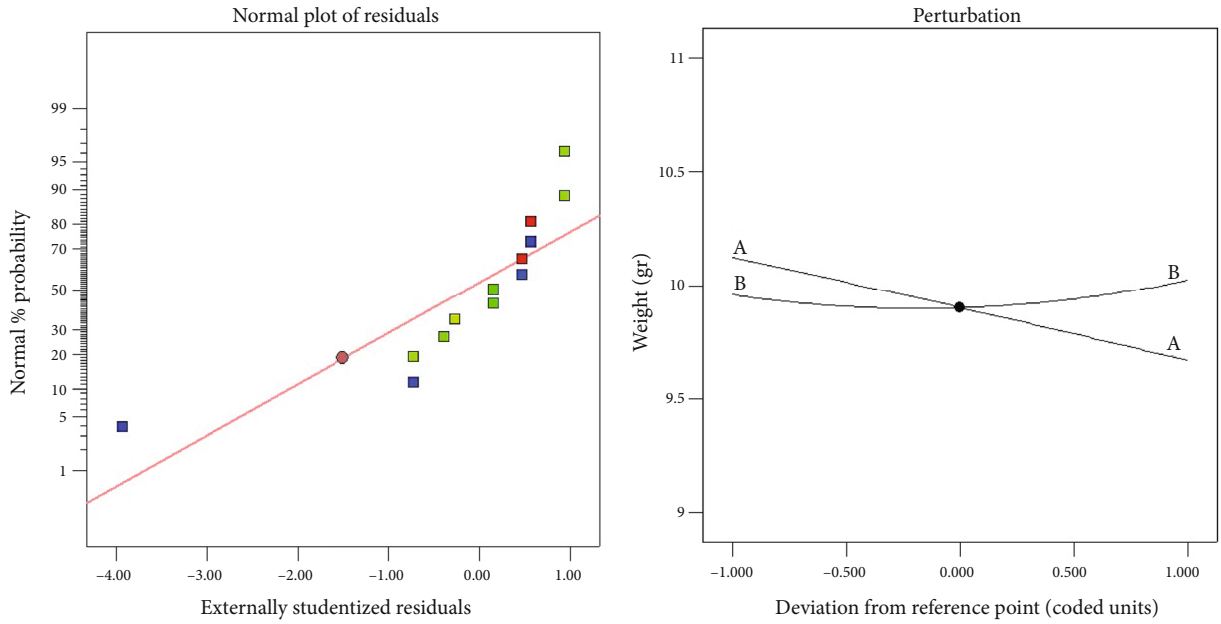


Figure 9: (a) Residuals' normal plot. (b) The plot of perturbation.

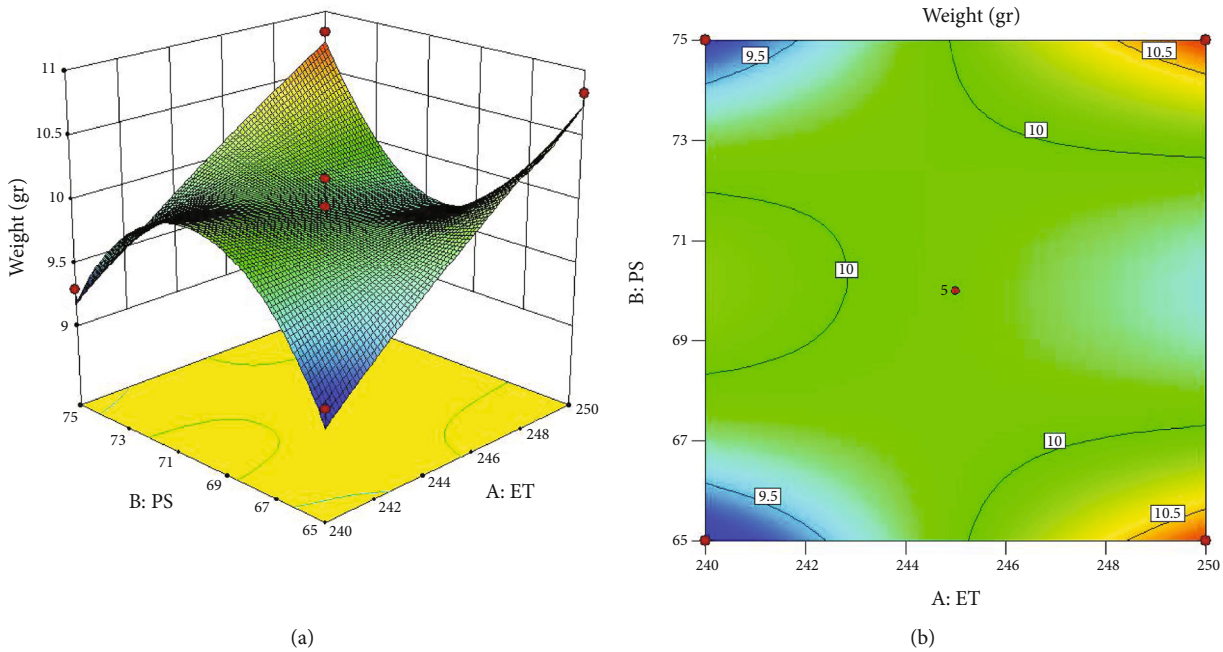


Figure 10: (a) The plot of response surface for weight output versus IP and pattern. (b) Contour plot IP and pattern.

controlling the input variables. The insights derived from the normal residual plot and perturbation graph contribute to an understanding of the correlation between the process parameters and the weight of the specimens.

In Figures 10(a) and 10(b), considering the effect of extruder temperature in the 3D-printed specimens, decreasing the extruder temperature decreases the weight of the specimens since the specimens do not possess high density. The output includes a graph with the $x$-axis (extension) and the $y$-axis (force). The elongation follows linearly up to a determined force, and the elongation continues to increase without changing the load. The force abruptly decreases when the sample breaks.

## 4. Optimization

The regression analysis included information regarding the lower and upper values of each variable, as presented in Table 8. According to the statistical analysis, the objective was to enhance both the most modulus and fracture

Table 8: Analysis regarding the minimum and maximum ranges of each variable.

| Variable | Aim | Limitations | | | | |
|---|---|---|---|---|---|---|
| | | Minimum limit | Maximum limit | Minimum weight | Maximum weight | Significance |
| A-ET | Within range | 240 | 250 | 1 | 1 | 3 |
| B-PS | Within range | 65 | 75 | 1 | 1 | 3 |
| Modulus | Maximize | 17.6771 | 26.5325 | 1 | 1 | 3 |
| Fracture elongation | Maximize | 2.57491 | 7.86669 | 1 | 1 | 3 |
| Weight | Minimize | 9.18 | 10.83 | 1 | 1 | 3 |

Table 9: Results of the statistical analysis.

| Number | Solutions | | | | | | |
|---|---|---|---|---|---|---|---|
| | ET | PS | Modulus | Fracture elongation | Weight | Desirability | |
| 1 | 247.038 | 69.525 | 25.302 | 5.320 | 9.809 | 0.598 | Selected |
| 2 | 244.039 | 65.000 | 25.597 | 5.087 | 9.794 | 0.580 | |
| 3 | 242.544 | 75.000 | 24.123 | 4.731 | 9.623 | 0.532 | |
| 4 | 242.847 | 75.000 | 23.928 | 4.812 | 9.674 | 0.532 | |

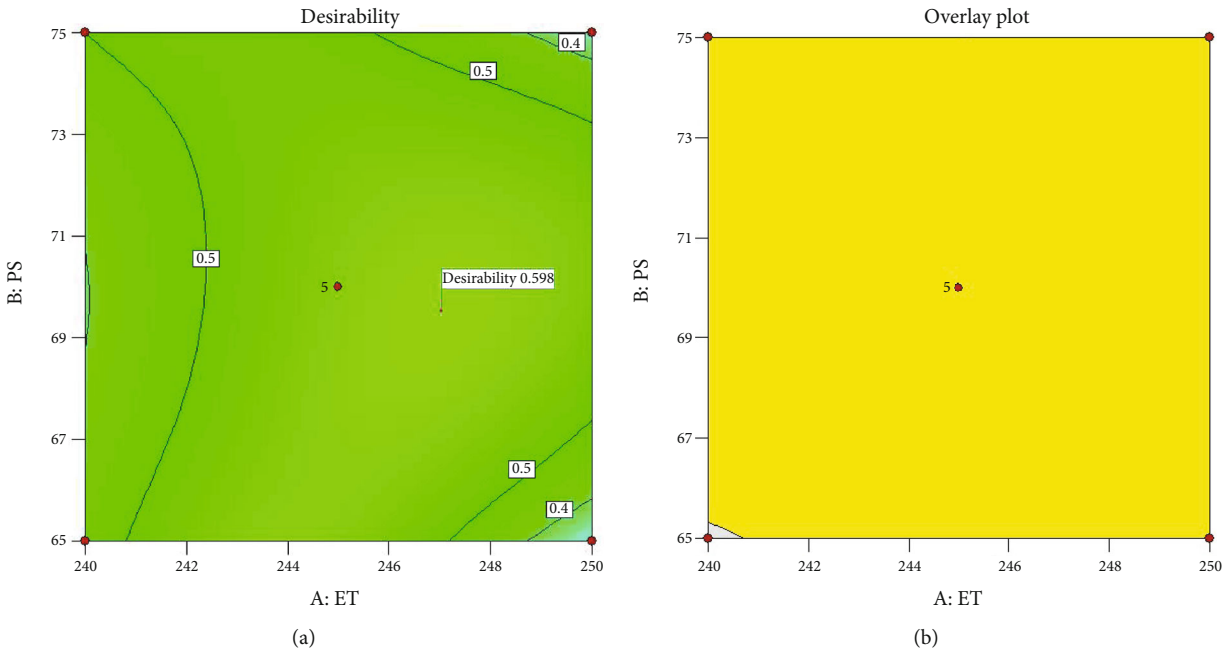


Figure 11: (a) Desirability and (b) overlay plot depicting pattern and intensity of the PVA 3D manufacturing.

elongation concurrently decreasing the weight. Table 9 presents the statistical analysis according to Table 2, identifying three specimens that exhibited specific characteristics. Additionally, Figure 11 displays an overlay plot, emphasizing the specimens situated within the optimal input variable regions highlighted in yellow. With reference to the statistical analysis and the use of the recommended specimens, there is an optimal balance among improved modulus and fracture elongation e concurrently degrading the weight.

## 5. Conclusion

Considering the previous findings on 3D printing of PA6-CF composites, the performance of these materials can be enhanced by altering the carbon fiber content, optimizing printing parameters, and refining heat treatment conditions. In this study, CarbonX (Gen3) PA6 carbon fiber-reinforced nylon filament, which is a relatively new filament and claimed to have good properties, was manufactured by FDM, in which two input variables, printing speed and the extruder temperature, were varied, and after doing tensile testing, the mechanical properties including modulus, elongation at tensile, fracture elongation, and the weight of parts were taken into account as responses for 11 parts in the RSM analysis approach. The most important results of this study are as follows:

The fiber-reinforced nylon filament properly could be printed by considering the effect of extruder temperature and printing speed.

Both printing speed and extruder temperature have an impact on the quality of 3D-printed parts.

Depending on the quality metric being taken into account (modulus, percent elongation, and component weight), the precise influence of printing speed and extruder temperature can change.

The outcomes may not be transferable to other procedures or materials because they depend on the particular conditions and materials employed in the 3D printing process.

Overall, the weight of the part varies between a minimum of 9.18 gm and a maximum of 10.83 gm.

The maximum modulus for the specimen reached 26.53 MPa, attributed to the continuity of the molten material enhancing this parameter. Consequently, raising the extruder temperature contributes to the improvement of the modulus.

An overlay plot was generated to illustrate the optimal states for the input variables.

Further experiments are needed to find out if the results can be generalized to other materials such as chopped or continuous fiber materials.

## Data Availability

No underlying data was collected or produced in this study.

## Disclosure

This study was conducted in an unbiased manner, and the findings are solely according to the data and evidence presented. The main aim of this research is to contribute to the scientific community's knowledge and promote further understanding in the respective field.

## Conflicts of Interest

There is no conflict of interest regarding the publication of this study. There are no financial or personal relationships with any individuals or organizations.

## Acknowledgments

The authors would like to extend their appreciation to the University of Northampton for providing the necessary resources, facilities, and funding that made this research possible. Additionally, the support and cooperation of the research team and laboratory staff (Paul Tallon, Aarokh Antonydas Shilaja Das, Jessica Shanai, Mohan Yadav, and Digvijay Patil) are deeply acknowledged for their assistance in data collection.

## References

[1] J. Abdullah and A. Y. Hassan, "Rapid prototyping in orthopaedics: principles and applications," in *Bone Grafts Bone Substitutes Basic*, pp. 547–561, Sci. Clin. Appl. (World Scientific Publishing Co), 2005.

[2] S. Upcraft and R. Fletcher, "The rapid prototyping technologies," *Assembly Automation*, vol. 23, no. 4, pp. 318–330, 2003.

[3] I. Gibson, D. Rosen, B. Stucker, I. Gibson, D. Rosen, and B. Stucker, "Extrusion-based systems," in *Additive Manufacturing Technologies*, pp. 147–173, Springer, New York, 2015.

[4] S. H. Huang, P. Liu, A. Mokasdar, and L. Hou, "Additive manufacturing and its societal impact: a literature review," *Journal of Advanced Manufacturing Technology*, vol. 67, no. 5-8, pp. 1191–1203, 2013.

[5] J. D. Kechagias, "Investigation of LOM process quality using design of experiments approach," *Rapid Prototyping Journal*, vol. 13, no. 5, pp. 316–323, 2007.

[6] J. D. Kechagias and S. P. Zaoutsos, "An investigation of the effects of ironing parameters on the surface and compression properties of material extrusion components utilizing a hybrid-modeling experimental approach," *Progress in Additive Manufacturing*, vol. 9, 2023.

[7] J. D. Kechagias and D. Chaidas, "Fused filament fabrication parameter adjustments for sustainable 3D printing," *Materials and Manufacturing Processes*, vol. 38, no. 8, pp. 933–940, 2023.

[8] J. Delgado, L. Serenó, K. Monroy, and J. Ciurana, "Selective laser sintering," in *Modern Manufacturing Processes*, pp. 481–499, Wiley, Hoboken, NJ, USA, 2019.

[9] C. Y. Yap, C. K. Chua, Z. L. Dong et al., "Review of selective laser melting: materials and applications," *Applied Physics Review*, vol. 2, no. 4, 2015.

[10] J. Zhang, B. Song, Q. Wei, I. D. Bourel, and Y. Shi, "A review of selective laser melting of aluminum alloys: processing, microstructure, property and developing trends," *Journal of Materials Science & Technology*, vol. 35, no. 2, pp. 270–284, 2019.

[11] H. R. Abedi, A. Z. Hanzaki, M. Azami, M. Kahnooji, and D. Rahmatabadi, "The high temperature flow behavior of additively manufactured Inconel 625 superalloy," *Materials Research Express*, vol. 6, no. 11, 2019.

[12] K. S. Boparai, R. Singh, and H. Singh, "Development of rapid tooling using fused deposition modeling: a review," *Rapid Prototyping Journal*, vol. 22, no. 2, pp. 281–299, 2016.

[13] H. K. Dave, B. H. Patel, S. R. Rajpurohit, A. R. Prajapati, and D. Nedelcu, "Effect of multi-infill patterns on tensile behavior of FDM printed parts," *Journal of the Brazilian Society of Mechanical Sciences and Engineering*, vol. 43, no. 1, pp. 1–15, 2021.

[14] M. S. Anoop, P. Senthil, and V. S. Sooraj, "An investigation on viscoelastic characteristics of 3D-printed FDM components using RVE numerical analysis," *Journal of the Brazilian Society of Mechanical Sciences and Engineering*, vol. 43, no. 1, pp. 1–13, 2021.

[15] M. S. Anoop and P. Senthil, "Homogenisation of elastic properties in FDM components using microscale RVE numerical analysis," *Journal of the Brazilian Society of Mechanical Sciences and Engineering*, vol. 41, no. 12, pp. 1–16, 2019.

[16] R. Hasanzadeh, P. Mihankhah, T. Azdast, M. Bodaghi, and M. Moradi, "Process-property relationship in polylactic acid composites reinforced by iron microparticles and3Dprinted by fused filament fabrication," *Polymer Engineering and Science*, vol. 64, no. 1, pp. 399–411, 2024.

[17] G. D. Goh, V. Dikshit, A. P. Nagalingam et al., "Characterization of mechanical properties and fracture mode of additively manufactured carbon fiber and glass fiber reinforced thermoplastics," *Materials and Design*, vol. 137, no. 5, pp. 79–89, 2018.

[18] M. N. Ahmad and A. R. Mohamad, "Analysis on dimensional accuracy of 3D printed parts by Taguchi approach," in

*Advances in Mechatronics, Manufacturing, and Mechanical Engineering. Lecture Notes in Mechanical Engineering*, M. Zakaria, A. Abdul Majeed, and M. Hassan, Eds., Springer, Singapore, 2021.

[19] M. Heidari-Rarani, M. Rafiee-Afarani, and A. M. Zahedi, "Mechanical characterization of FDM 3D printing of continuous carbon fiber reinforced PLA composites," *Composites Part B: Engineering*, vol. 175, no. 15, article 107147, 2019.

[20] H. J. Um, J. S. Lee, J. H. Shin, and H. S. Kim, "3D printed continuous carbon fiber reinforced thermoplastic composite sandwich structure with corrugated core for high stiffness/load capability," *Composite Structures*, vol. 291, no. 1, article 115590, 2022.

[21] H. Tang, Q. Sun, Z. Li, X. Su, and W. Yan, "Longitudinal compression failure of 3D printed continuous carbon fiber reinforced composites: an experimental and computational study," *Composites Part A: Applied Science and Manufacturing*, vol. 146, p. 106416, 2021.

[22] W. Chen, Q. Zhang, H. Cao, and Y. Yuan, "Process evaluation, tensile properties, mathematical models, and fracture behavior of 3D printed continuous fiber reinforced thermoplastic composites," *Journal of Reinforced Plastics and Composites*, vol. 40, no. 21-22, pp. 845–863, 2021.

[23] X. Tian, T. Liu, C. Yang, Q. Wang, and D. Li, "Interface and performance of 3D printed continuous carbon fiber reinforced PLA composites," *Composites Part A: Applied Science and Manufacturing*, vol. 88, pp. 198–205, 2016.

[24] L. G. Blok, M. L. Longana, H. Yu, and B. K. S. Woods, "An investigation into 3D printing of fibre reinforced thermoplastic composites," *Additive Manufacturing*, vol. 22, pp. 176–186, 2018.

[25] S. Bhandari, R. A. Lopez-Anido, and D. J. Gardner, "Enhancing the interlayer tensile strength of 3D printed short carbon fiber reinforced PETG and PLA composites via annealing," *Additive Manufacturing*, vol. 30, p. 100922, 2019.

[26] M. Moradi, A. Aminzadeh, D. Rahmatabadi, and A. Hakimi, "Experimental investigation on mechanical characterization of 3D printed PLA produced by fused deposition modeling (FDM)," *Materials Research Express*, vol. 8, no. 3, article 035304, 2021.

[27] M. Nazri Ahmad, M. Ridzwan Ishak, M. T. Mastura, Z. Leman, and F. Mustapha, "Rheological properties of natural fiber reinforced thermoplastic composite for fused deposition modeling (FDM): a short review," *Journal of Advanced Research in Fluid Mechanics and Thermal Sciences*, vol. 98, no. 2, pp. 157–164, 2022.

[28] V. Panwar, D. Kumar Sharma, K. V. Pradeep Kumar, A. Jain, and C. Thakar, "Experimental investigations and optimization of surface rough-ness in turning of EN 36 alloy steel using response surface methodology and genetic algorithm," *Materials Today Proceedings*, vol. 46, pp. 6474–6481, 2021.

[29] M. Abdellatief, W. E. Elemam, H. Alanazi, and A. M. Tahwia, "Production and optimization of sustainable cement brick incorporating clay brick wastes using response surface method," *Ceramics International*, vol. 49, no. 6, pp. 9395–9411, 2023.

[30] B. S. Mohammed and M. Adamu, "Mechanical performance of roller compacted concrete pavement containing crumb rubber and nano silica," *Construction and Building Materials*, vol. 159, pp. 234–251, 2018.

[31] R. H. Myers, D. C. Montgomery, G. G. Vining, C. M. Borror, and S. M. Kowalski, "Response surface methodology: a retrospective and literature survey," *Journal of Quality Technology*, vol. 36, no. 1, pp. 53–77, 2004.

[32] M. A. Bezerra, R. E. Santelli, E. P. Oliveira, L. S. Villar, and L. A. Escaleira, "Response surface methodology (RSM) as a tool for op-timization in analytical chemistry," *Talanta*, vol. 76, no. 5, pp. 965–977, 2008.

[33] I. M. Alarifi, "A performance evaluation study of 3d printed nylon/glass fiber and nylon/carbon fiber composite materials," *Journal of Materials Research and Technology*, vol. 21, pp. 884–892, 2022.